Amino Acids (2017) 49:895–903
DOI 10.1007/s00726-017-2387-4

ORIGINAL ARTICLE

A novel BRET-based binding assay for interaction studies of relaxin family peptide receptor 3 with its ligands

Jia-Hui Wang[1] · Xiao-Xia Shao[1] · Meng-Jun Hu[1] · Dian Wei[1] · Ya-Li Liu[1] · Zeng-Guang Xu[1] · Zhan-Yun Guo[1]

Received: 10 January 2017 / Accepted: 27 January 2017 / Published online: 4 February 2017

Abstract Relaxin family peptide receptor 3 (RXFP3) is an A-class G protein-coupled receptor that is implicated in the regulation of food intake and stress response upon activation by its cognate agonist relaxin-3. To study its interaction with various ligands, we developed a novel bioluminescence resonance energy transfer (BRET)-based binding assay using the brightest NanoLuc as an energy donor and a newly developed cyan-excitable orange fluorescent protein (CyOFP) as an energy acceptor. An engineered CyOFP without intrinsic cysteine residues but with an introduced cysteine at the C-terminus was overexpressed in *Escherichia coli* and chemically conjugated to the A-chain N-terminus of an easily labeled chimeric R3/I5 peptide via an intermolecular disulfide linkage. After the CyOFP-conjugated R3/I5 bound to a shortened human RXFP3 (removal of 33 N-terminal residues) fused with the NanoLuc reporter at the N-terminus, high BRET signals were detected. Saturation binding and real-time binding assays demonstrated that this BRET pair retained high binding affinity with fast association/dissociation. Using this BRET pair, binding potencies of various ligands with RXFP3 were conveniently measured through competition binding assays. Thus, the novel BRET-based binding assay facilitates interaction studies of RXFP3 with various ligands. The engineered CyOFP without intrinsic cysteine residues may also be applied to other BRET-based binding assays in future studies.

Keywords BRET · RXFP3 · Relaxin-3 · Interaction · Binding

Introduction

The relaxin family is a group of peptide hormones, including relaxin (primates express two relaxins, namely relaxin-1 and relaxin-2), relaxin-3 (also known as INSL7), and insulin-like peptide 3–6 (INSL3, INSL4, INSL5, and INSL6) (Bathgate et al. 2013a; Callander and Bathgate 2010; Halls et al. 2015). The relaxin family is a branch of the insulin superfamily which also includes insulin and insulin-like growth factor 1 and 2 (IGF-1 and IGF-2). The relaxin family peptides play a variety of biological functions, such as regulation of reproduction, food intake, stress response, and glucose homeostasis. So far, four formerly orphan G protein-coupled receptors (GPCRs) have been identified as their receptors, namely relaxin family peptide receptor 1–4 (RXFP1–4). Relaxin and INSL3 are the cognate agonists of the homologous RXFP1 and RXFP2, respectively (Hsu et al. 2002; Kumagai et al. 2002). Relaxin-3 and INSL5 are the cognate agonists of the homologous RXFP3 and RXFP4, respectively (Liu et al. 2003b, 2005b). In addition, relaxin-3 can activate RXFP1 and RXFP4 in vitro with high efficiency (Liu et al. 2003a; Sudo et al. 2003).

Both RXFP3 and its cognate agonist relaxin-3 are primarily expressed in the brain and this receptor–ligand pair is implicated in the regulation of food intake, stress response, arousal and exploratory behaviors (Calvez et al. 2016; Kumar et al. 2016; Ma et al. 2016; Smith et al. 2015; Zhang et al. 2015). Thus, RXFP3 is a potential therapeutic

Electronic supplementary material The online version of this article (doi:10.1007/s00726-017-2387-4) contains supplementary material, which is available to authorized users.

✉ Zhan-Yun Guo
zhan-yun.guo@tongji.edu.cn

[1] Research Center for Translational Medicine at East Hospital, College of Life Sciences and Technology, Tongji University, Shanghai, China

target for obesity and anxiety, and several synthetic agonists and antagonists have been generated in recent studies. The designed agonists include the chimeric R3/I5 (containing the B-chain of relaxin-3 and the A-chain of INSL5) (Liu et al. 2005a), simplified relaxin-3 analogs (Shabanpoor et al. 2012), and stapled relaxin-3 B-chain analogs (Hojo et al. 2016; Jayakody et al. 2016), while the designed antagonists include the chimeric R3(BΔ23-27)R/I5 (Kuei et al. 2007), [G(B23)A,G(B24)S]R3/I5 (Hu et al. 2016a), and the shortened B-chain analog R3B1-22R (Haugaard-Kedström et al. 2011).

Ligand–receptor binding assays are widely used to characterize the natural or designed ligands or screen novel ones. Conventionally, the binding assays rely on highly sensitive tracers (Bylund and Toews 2011; Hulme and Trevethick 2010; Maguire et al. 2012). For example, iodine-125 (^{125}I)-labeled relaxin-3 and R3/I5 have been used as radioactive tracers for ligand-binding assays of RXFP3 (Liu et al. 2003b, 2005a). Europium (Eu^{3+})-labeled fluorescent tracers and NanoLuc-conjugated bioluminescent tracers have also been developed for interaction studies of RXFP3 with ligands (Hu et al. 2016b; Liu and Guo 2016; Shabanpoor et al. 2011; Zhang et al. 2012a, b, 2013a, b). However, the conventional binding assays include a necessary but time-consuming washing step to remove unbound tracer before measurement of the bound tracer. In recent studies, novel bioluminescence resonance energy transfer (BRET)-based ligand–receptor binding assays have been developed using the brightest NanoLuc as an energy donor (Machleidt et al. 2015; Soave et al. 2016; Stoddart et al. 2015). BRET-based binding assays do not require the washing step because unbound tracer does not interfere with measurement of the receptor-bound tracer. Thus, the BRET-based ligand–receptor binding assay is convenient for use and compatible with high throughput screening.

To obtain high BRET signals with low background, an appropriate energy acceptor is needed for the NanoLuc reporter that has the brightest bioluminescence reported to date (Hall et al. 2012). The excitation spectrum of the energy acceptor should overlap as much as possible with the emission spectrum of NanoLuc for efficient energy transfer, while the emission spectrum of the acceptor should be as different as possible from the emission spectrum of NanoLuc to reduce interference from NanoLuc emission. In a recent study, a cyan-excitable orange fluorescent protein (CyOFP) with a large Stokes shift was developed as an improved energy acceptor for NanoLuc (Chu et al. 2016). In the present work, we applied the newly developed CyOFP to bimolecular interaction studies and developed a novel BRET-based ligand-binding assay for receptor RXFP3 to facilitate its interaction studies with various ligands.

Materials and methods

Generation of expression constructs for N-terminally NanoLuc-fused RXFP3s

The coding region of the secretory NanoLuc, carrying the signal peptide of human interleukin-6, was PCR amplified using the vector pNL1.3 (Promega, Madison, WI, USA) as the template. After cleavage by restriction enzymes *Nhe*I and *Kpn*I, the amplified DNA fragment was ligated into vector pcDNA6, resulting in the construct pcDNA6/sLuc. The coding regions of human RXFP3 with or without N-terminal deletions were PCR amplified using the expression construct pcDNA6/RXFP3 as the template. After cleavage by restriction enzymes *Kpn*I and *Age*I, the amplified DNA fragments were ligated into vector pcDNA6/sLuc, resulting in expression constructs for N-terminally NanoLuc-fused RXFP3s with or without deletions from the N-terminus of human RXFP3. Nucleotide sequences of the NanoLuc-fused RXFP3s were confirmed by DNA sequencing.

Generation of expression constructs for engineered CyOFPs

The coding region of the wild-type CyOFP1 (amino acids 1–225) was chemically synthesized according to the published sequence (Chu et al. 2016). After cleavage by restriction enzymes *Nde*I and *Eco*RI, the synthetic DNA fragment was ligated into a pET vector that encodes an N-terminal 6×His-tag and a C-terminal long arm (21 amino acids) with a terminal Cys residue, resulting in the expression construct pET/6×His-CyOFP-L-Cys. To generate expression constructs for mutant CyOFPs with the intrinsic Cys residues replaced by Ser or Ala, site-directed mutagenesis was conducted through the QuikChange method using pET/6×His-CyOFP-L-Cys as the template. To change the long C-terminal arm for a short one (12 amino acids), the expression construct pET/6×His-[C1A,C2A]CyOFP-L-Cys was cleaved by restriction enzymes *Eco*RI and *Not*I and then ligated with a short synthetic DNA fragment encoding the short arm, resulting in the expression construct pET/6×His-[C1A,C2A]CyOFP-S-Cys. The nucleotide sequences of the wild-type and engineered CyOFPs were confirmed by DNA sequencing.

Overexpression and purification of the engineered CyOFPs

The CyOFP expression constructs were, respectively, transformed into *Escherichia coli* strain BL21(DE3). Thereafter, the transformants were cultured in liquid Luria–Bertani

both (supplemented with 100 mg/l of ampicillin) to OD_{600} ≈1.0 at 37 °C and then induced with 1.0 mM isopropyl β-D-1-thiogalactopyranoside at 25 °C for ~10 h. Expression of CyOFP was preliminarily judged by the color of the cell pellet and confirmed by SDS-PAGE. After the *E. coli* cells were lysed by sonication in lysis buffer (50 mM phosphate buffer, pH 7.5, 0.5 M NaCl), the supernatant was subjected to S-sulfonation by addition of urea, sodium sulfite (Na_2SO_3), and sodium tetrathionate ($Na_2S_4O_6$) to final concentrations of 8.0 M, 100 mM, and 80 mM, respectively. After shaking at room temperature for ~2 h, the lysate supernatant was applied to an immobilized Ni^{2+} affinity chromatography column and the S-sulfonated CyOFP was eluted with 250 mM imidazole in lysis buffer plus 8.0 M urea. Thereafter, the eluted CyOFP fraction was treated with 50 mM dithiothreitol (DTT) at room temperature for ~30 min, and then loaded onto a gel filtration column (TSKgel G2000SW_{XL}, 7.8 mm × 300 mm; Sigma Aldrich, St. Louis, MO, USA). The CyOFP fraction was then eluted from the gel filtration column with 50 mM phosphate buffer (pH 7.5), analyzed by SDS-PAGE, and quantified by absorbance at 500 nm using the extinction coefficient of 40 mM^{-1} cm^{-1} as reported (Chu et al. 2016).

Preparation of relaxin family peptides

The easily labeled R3/I5 peptide and human INSL5 were prepared according to our previous procedures (Luo et al. 2010; Zhang et al. 2013b). Briefly, they were overexpressed in *E. coli* as single-chain precursors and then subjected to in vitro refolding and enzymatic maturation. The mature peptides were purified to homogeneity by high performance liquid chromatography (HPLC) using a C18 reverse-phase column (Zorbax 300SB-C18, 4.6 × 250 mm; Agilent Technology, Santa Clara, CA, USA) and their molecular masses were confirmed by mass spectrometry.

Chemical conjugation of the engineered CyOFPs with the easily labeled R3/I5

The purified easily labeled R3/I5 peptide was first treated with bifunctional reagent *N*-succinimidyl 3-(2-pyridyldithio)propionate (SPDP) according to our previous procedure (Hu et al. 2016b; Zhang et al. 2013a). The SPDP-modified peptide was purified by HPLC using a C18 reverse-phase column (Zorbax 300SB-C18, 4.6 × 250 mm, from Agilent) and confirmed by mass spectrometry. For chemical conjugation, one volume of the engineered CyOFP fraction (eluted from the gel filtration column, ~50 μM) was sequentially mixed with one volume of the SPDP-modified R3/I5 (dissolved in 1.0 mM aqueous hydrochloride, ~150 μM) and a one-third volume of 8 M urea solution. After incubation at 30 °C for 30 min, the conjugation mixture was loaded onto a small home-made spin Ni^{2+} column containing ~50 μl affinity resin. After washing with washing buffer (50 mM phosphate buffer, pH 7.5), the conjugate was eluted from the spin column with 250 mM imidazole in washing buffer. Total CyOFP in the eluted fraction was quantified by fluorometry using the purified engineered CyOFP as a standard. The conjugate percentage in the eluted fraction was estimated from band density on SDS-PAGE.

BRET-based ligand-binding assays for RXFP3

The expression constructs for the NanoLuc-fused RXFP3s were transiently transfected into human embryonic kidney (HEK) 293T cells. After transfection for ~36 h, the cells were treated with 1.0 mM ethylenediaminetetraacetic acid [in phosphate-buffered saline (PBS)] and the suspended cells were collected by centrifugation (800*g*, 2 min). After washed with PBS, the cells were resuspended in binding solution (serum-free Dulbecco's modified Eagle's medium plus 1% bovine serum albumin). Thereafter, the cell suspension was divided into a white opaque 96-well plate (20 μl/well, ~5 × 10^4 cells/well). For saturation binding assays, the cells were mixed with binding solution (20 μl/well) containing varied concentrations of CyOFP-conjugated R3/I5. For competition binding assays, the cells were mixed with binding solution (20 μl/well) containing a constant concentration of CyOFP-conjugated R3/I5 and varied concentrations of competitor. After incubation at 20 °C for ~20 min, NanoLuc substrate was added (1 μl/well) and BRET was immediately measured using a GloMax Discover plate reader (Promega). For real-time binding assays, the cells were sequentially mixed with 1 μl of NanoLuc substrate and 20 μl of binding solution containing 20 nM of CyOFP-conjugated R3/I5, and BRET data were collected at an interval of ~0.5 min for ~10 min. Thereafter, 1 μl of 4 μM R3/I5 stock solution was added and BRET data were continuously collected at an interval of ~0.5 min for ~10 min.

Results and discussion

Preparation of engineered CyOFPs for conjugation with R3/I5

To develop a BRET-based ligand-binding assay for RXFP3, we attempted to conjugate the newly developed CyOFP with the chimeric R3/I5 peptide that retains high binding affinity with RXFP3, but has lower nonspecific binding compared to the cognate ligand relaxin-3 (Liu et al. 2005a). For convenient conjugation, we added a long arm with a terminal Cys residue (amino acid sequence

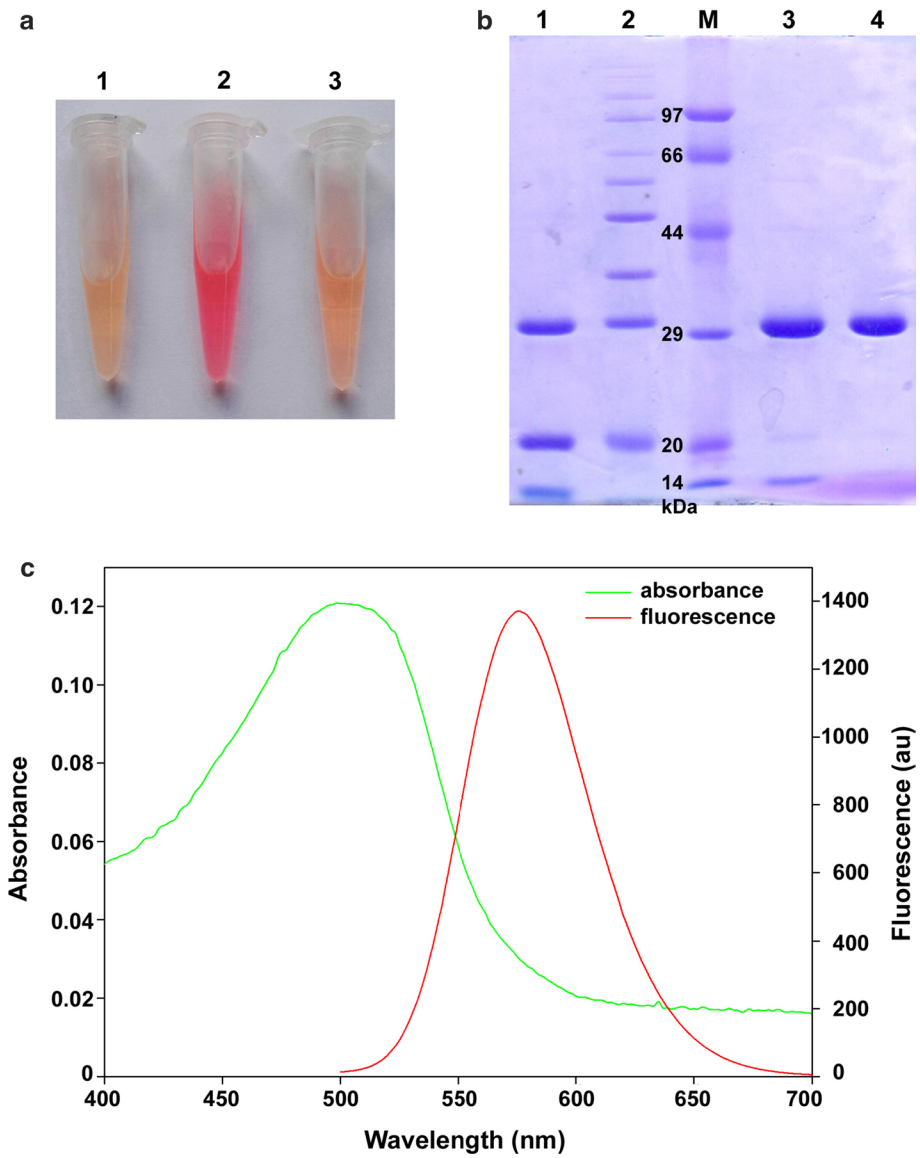

Fig. 1 Characterization of the engineered CyOFP. **a** Photograph of 6×His-[C1A,C2A] CyOFP-L-Cys fractions. *Tube 1* supernatant of the *E. coli* lysate, *tube 2* fraction from the Ni^{2+} column, *tube 3* fraction from the gel filtration column. **b** SDS-PAGE analysis of 6×His-[C1A,C2A]CyOFP-L-Cys fractions. *Lane 1* fraction from Ni^{2+} column boiled in SDS loading buffer without reducing reagents, *lane 2* fraction from gel filtration column boiled in SDS loading buffer without reducing reagents, *lane 3* fraction from Ni^{2+} column boiled in SDS loading buffer containing 50 mM DTT, *lane 4* fraction from gel filtration column boiled in SDS loading buffer containing 50 mM DTT. After boiling for 3–5 min in the SDS loading buffer, an appropriate amount (~2 μg) of samples was loaded onto a 12% SDS-gel. After electrophoresis, the gel was stained by Coomassie Brilliant Blue R250. **c** Absorption and emission spectra of the purified 6×His-[C1A,C2A] CyOFP-L-Cys. The engineered CyOFP was diluted into 20 mM phosphate buffer (pH 7.5) to the final concentration of ~3 μM and then absorbance spectrum and fluorescence spectrum (excitation at 470 nm) were measured on a photometer and a fluorometer

GGSNSGGGSGGGSGGGGGGGC) to the C-terminus of wild-type CyOFP. For convenient purification, we introduced a 6×His-tag to the N-terminus. The resultant 6×His-CyOFP-L-Cys (nucleotide and amino acid sequences shown in Supplementary Fig. S1) was efficiently overexpressed in *E. coli* as a soluble protein with orange color, suggesting correct formation of the fluorescent chromophore.

Unfortunately, the wild-type CyOFP contains two intrinsic Cys residues that interfered with chemical conjugation in subsequent experiments. Thus, we attempted to replace them with Ser or Ala residues. Ser replacement of the N-terminal Cys residue (C1) likely disturbed formation of the fluorescent chromophore, because the overexpressed mutant protein was colorless. However, replacement of the N-terminal Cys residue with Ala likely had no detriments because the mutant protein was normally overexpressed and orange. The intrinsic C-terminal Cys residue (C2) of CyOFP was tolerant to both Ser and Ala replacement. Thus, we replaced both intrinsic Cys residues of CyOFP with Ala, and the resultant 6×His-[C1A,C2A]CyOFP-L-Cys lacks intrinsic Cys residues but has a single introduced Cys residue at the C-terminus.

The engineered 6×His-[C1A,C2A]CyOFP-L-Cys was overexpressed in *E. coli* as a soluble orange protein (Fig. 1a, tube 1). To prevent formation of intermolecular disulfide linkages, the supernatant of the cell lysate was subjected to S-sulfonation that reversibly blocked the sulfhydryl moiety of the single Cys residue with a sulfonate group. After loading onto a Ni^{2+} column, the eluted fraction was pink (Fig. 1a, tube 2), likely owing to the presence of imidazole and urea in the eluent. As analyzed by SDS-PAGE, the eluted fraction displayed a major band (~29 kDa) after the sample was boiled in SDS loading buffer with DTT (Fig. 1b,

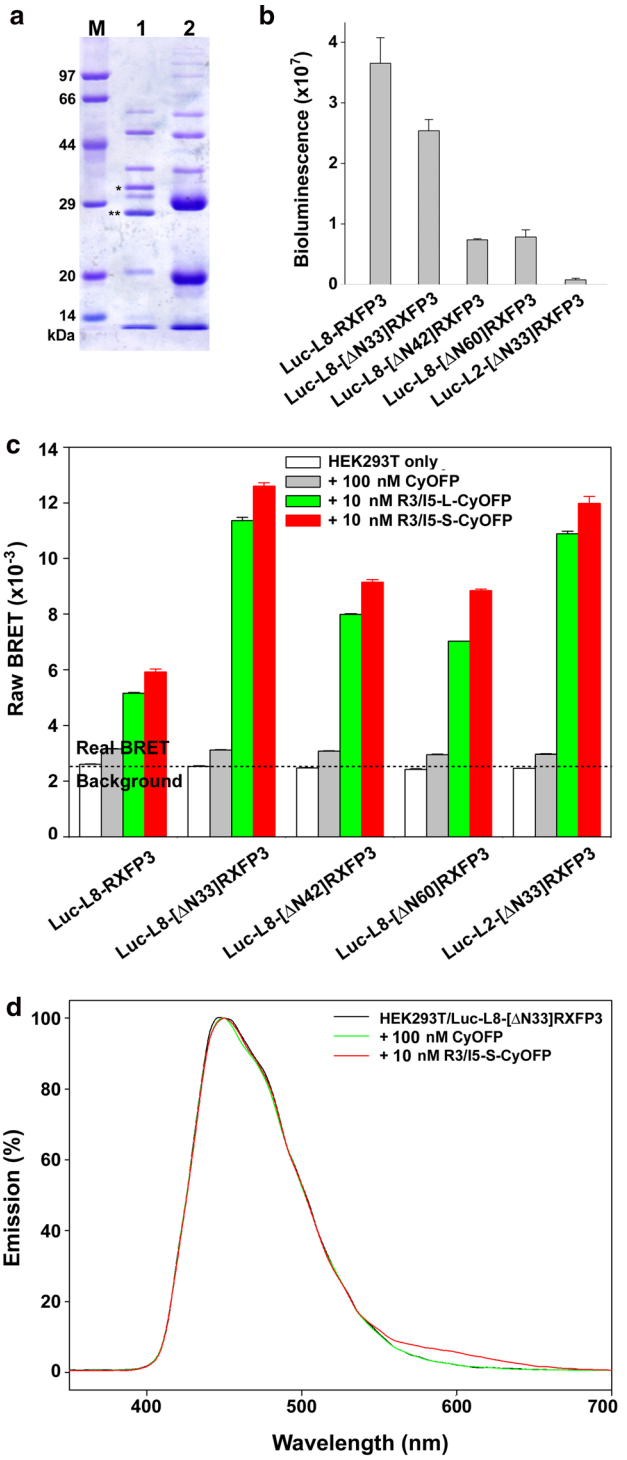

Fig. 2 Optimization of the BRET measurement. **a** SDS-PAGE analysis of the conjugate of R3/I5 with 6×His-[C1A,C2A]CyOFP-L-Cys. *Lane 1* fraction eluted from the spin Ni^{2+} column, *lane 2* the purified 6×His-[C1A,C2A]CyOFP-L-Cys. The samples were boiled for 3–5 min in SDS loading buffer without reducing reagents and then loaded onto a 15% SDS-gel. After electrophoresis, the gel was stained by Coomassie Brilliant Blue R250. **b** Bioluminescence of the HEK293T cells overexpressing various constructs of the NanoLuc-fused RXFP3s. The data were expressed as mean ± standard error (SE) ($n = 3$). **c** Raw BRET data measured after the HEK293T cells overexpressing NanoLuc-fused RXFP3s were preincubated with the CyOFP-conjugated R3/I5 tracers. The data were expressed as mean ± SE ($n = 3$). **d** Emission spectra of HEK293 cells overexpressing Luc-L8-[ΔN33]RXFP3 with or without preincubation with R3/I5-S-CyOFP or CyOFP. The spectra were recorded on a SpectraMax M5 plate reader (Molecular Devices)

lane 3), consistent with the expected value (28.5 kDa) of intact 6×His-[C1A,C2A]CyOFP-L-Cys. Thus, intact engineered CyOFP was obtained after overexpression and purification. However, a smaller band (~20 kDa) also appeared on SDS-PAGE after the sample was boiled in SDS loading buffer without reducing agents (Fig. 1b, lane 1). This phenomenon has been observed in some red fluorescent proteins (CyOFP was developed from a red fluorescent protein) and is caused by peptide chain breakage due to hydrolysis of the acylimine bond of the red chromophore (Gross et al. 2000; Subach et al. 2010; Yarbrough et al. 2001). Thus, we deduced that the ~20 kDa band was the hydrolyzed C-terminal fragment (19.1 kDa in theory) of the engineered CyOFP. The hydrolyzed N-terminal fragment (9.4 kDa in theory) could also be observed on SDS-PAGE using a higher percentage gel (Fig. 2a).

The fraction eluted from the Ni^{2+} column was then treated with DTT to remove the sulfonate moiety from the Cys residue of the engineered CyOFP. After eluted from a gel filtration column, the engineered CyOFP was again orange (Fig. 1c, tube 3). This eluted fraction displayed a single band (~29 kDa) on SDS-PAGE if the sample was boiled in SDS loading buffer with DTT (Fig. 1b, lane 4), suggesting that homogenous engineered CyOFP was obtained. However, a series of bands appeared on SDS-PAGE if the sample was boiled in SDS loading buffer without reducing agents (Fig. 1b, lane 2). As discussed above, the ~20 kDa band was the hydrolyzed C-terminal fragment that carries a free Cys residue. The ~40-, ~50-, and ~60 kDa bands likely represented disulfide-crosslinked homodimers and heterodimers of the hydrolyzed C-terminal fragment and intact 6×His-[C1A,C2A]CyOFP-L-Cys. Other larger bands likely represented non-covalent aggregates of the disulfide-crosslinked dimers. If the sample was loaded onto the gel without boiling, a smear band with an apparent molecular weight of ~60 kDa appeared on SDS-PAGE whether or not reducing reagents were present in the SDS loading buffer, suggesting that the engineered CyOFP formed noncovalent dimers in SDS gels without boiling of the sample before loading. Thus, CyOFP displayed strange behavior on SDS-PAGE if it was not boiled in SDS loading buffer with high concentration of DTT (50 mM in our experiments).

To test whether mutation of two intrinsic Cys residues affected the fluorescence properties of CyOFP, we

measured the absorption and emission spectra of purified 6×His-[C1A,C2A]CyOFP-L-Cys. As shown in Fig. 1c, the engineered CyOFP displayed a broad absorption peak around 480–520 nm and an emission peak around 580–590 nm after excitation at 470 nm, consistent with the reported values for wild-type CyOFP (Chu et al. 2016). Thus, replacement of the intrinsic Cys residues did not affect the fluorescence properties of CyOFP.

To test the effect of the length of the C-terminal arm on the BRET efficiency, we also generated an engineered CyOFP carrying a short C-terminal arm (amino acid sequence GGSNSGGGGGGGC). The resultant 6×His-[C1A,C2A]CyOFP-S-Cys was overexpressed and purified according to the procedure above and displayed almost the same properties as 6×His-[C1A,C2A]CyOFP-L-Cys.

Conjugation of the engineered CyOFPs with R3/I5 and improvement of BRET efficiency

To conjugate the engineered CyOFPs with the easily labeled R3/I5 peptide, we used a two-step procedure that was developed for conjugation of the NanoLuc reporter with relaxin family peptides in our previous studies (Hu et al. 2016b; Zhang et al. 2013a). First, an active disulfide bond was introduced to the A-chain N-terminus of the easily labeled R3/I5 through chemical modification with bifunctional reagent SPDP that carries a primary amine-specific *N*-hydroxysuccinimidyl ester and an active disulfide bond. Thereafter, the engineered CyOFP was reacted with the SPDP-modified R3/I5: the unique C-terminal Cys residue of the engineered CyOFP would react with the active disulfide bond of the SPDP-modified R3/I5 and thus form an intermolecular disulfide linkage. To remove unconjugated R3/I5 peptide that would interfere with subsequent receptor-binding of the conjugate, the conjugation mixture was subjected to a small Ni^{2+} spin column that could bind the conjugate and the unconjugated CyOFP, but could not bind the unconjugated R3/I5. As analyzed by SDS-PAGE (Fig. 2a), the eluted fraction (lane 1) displayed two additional bands (indicated by asterisks) compared to the purified 6×His-[C1A,C2A]CyOFP-L-Cys itself (lane 2) after both of them were boiled in SDS loading buffer without reducing reagents before loading. We deduced that the additional band indicated by one asterisk represented the intact conjugate (designated R3/I5-L-CyOFP), because it was larger than the band of intact, monomeric CyOFP. The smaller additional band (indicated by a double asterisk) probably arose from hydrolysis of the engineered CyOFP in the intact conjugate during boiling of the sample before loading. Thus, both of the additional bands represented the conjugate. Estimated from band densities (Fig. 2a), the conjugate accounted for ~50% in the eluted fraction. Similar results were obtained for conjugation of the purified 6×His-[C1A,C2A]CyOFP-S-Cys with R3/I5. Since unconjugated CyOFP had almost no effect on the BRET assay (Fig. 2c), the conjugate fraction was not further purified, although it contained ~50% of unconjugated CyOFP.

To use NanoLuc as an energy donor for the BRET-based ligand-binding assay, we genetically fused a secretory NanoLuc (with the signal peptide of human interleukin 6) to the N-terminus of human RXFP3 through a linker peptide of eight residues (amino acid sequence SSGGGGGT). After the resultant Luc-L8-RXFP3 construct was transiently overexpressed in HEK293T cells, strong bioluminescence was detected (Fig. 2b), suggesting efficient expression of the fusion protein in the transfected cells. After these cells were incubated with the conjugate R3/I5-L-CyOFP or R3/I5-S-CyOFP, low but significant BRET signals were detected (Fig. 2c), suggesting that the CyOFP-conjugated R3/I5 could bind to the NanoLuc-fused RXFP3. In contrast, almost no BRET was detected after these cells were incubated with the engineered CyOFP, suggesting that CyOFP itself could not bind to RXFP3.

To improve the BRET efficiency, we tried shortening the extracellular N-terminus of RXFP3. A previous study has demonstrated that the N-terminal 33 residues of human RXFP3 are not important for the receptor function (Bathgate et al. 2013b); thus, we first removed this fragment from human RXFP3. The resultant Luc-L8-[ΔN33]RXFP3 was almost normally expressed in transfected HEK293T cells (Fig. 2b) and displayed much higher BRET efficiency with both tracers (Fig. 2c). However, removal of more N-terminal residues impaired both expressions of the NanoLuc-fused receptors (Fig. 2b) and their BRET efficiency with the fluorescent tracers (Fig. 2c). A shorter linker (a Thr-Gly dipeptide) between NanoLuc and [ΔN33]RXFP3 seriously affected expression of the construct in HEK293T cells (Fig. 2b), although the construct retained high BRET efficiency with the fluorescent tracers (Fig. 2c). Thus, Luc-L8-[ΔN33]RXFP3 was the best receptor construct for BRET assay with the CyOFP-based fluorescent tracers.

For these NanoLuc-fused RXFP3 constructs, R3/I5-S-CyOFP displayed slightly higher BRET efficiency than R3/I5-L-CyOFP (Fig. 2c). Thus, we used R3/I5-S-CyOFP and Luc-L8-[ΔN33]RXFP3 as a BRET pair in later experiments. As shown in Fig. 2d, Luc-L8-[ΔN33]RXFP3 displayed a broad emission spectrum with a peak at ~460 nm after addition of the NanoLuc substrate to living HEK293T cells overexpressing this construct. After these cells were preincubated with R3/I5-S-CyOFP, the emission spectrum around 570–650 nm was significantly increased, confirming energy transfer from the receptor-fused NanoLuc to the ligand-conjugated CyOFP after ligand–receptor binding. In contrast, preincubation with the engineered CyOFP itself

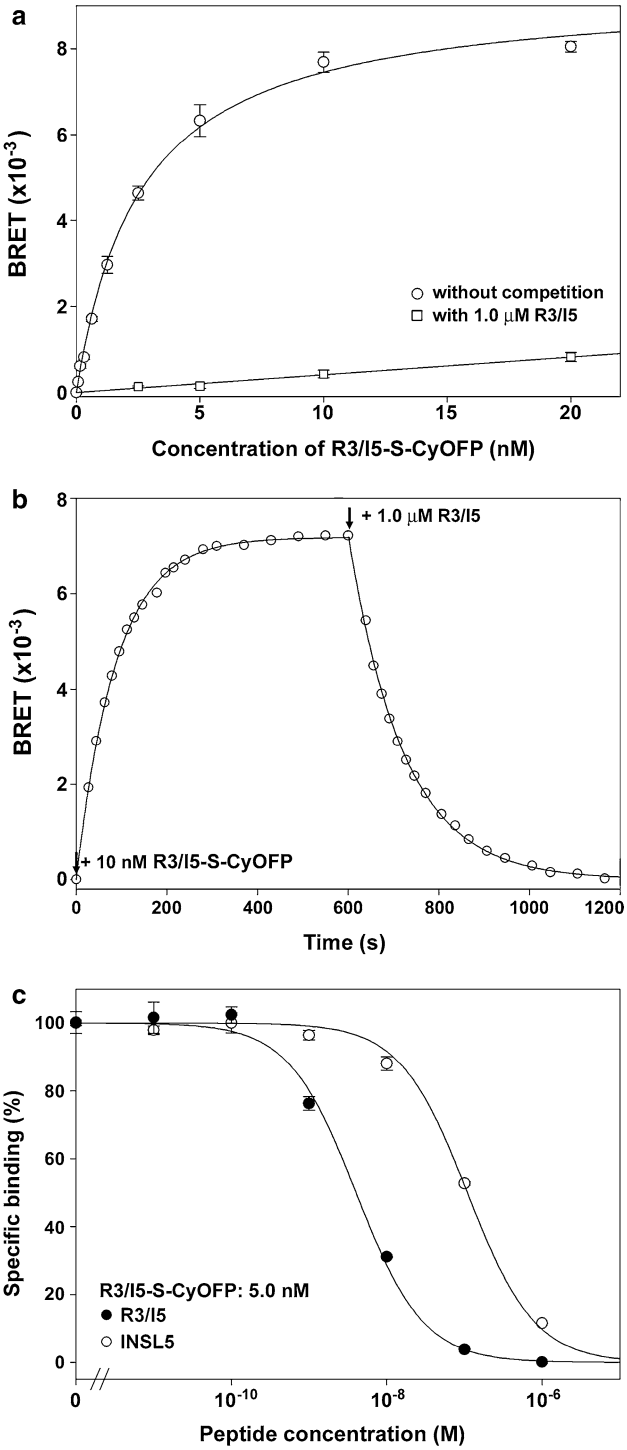

Fig. 3 BRET-based ligand-binding assays for RXFP3. **a** Saturation binding of R3/I5-S-CyOFP with living HEK293T cells overexpressing Luc-L8-[ΔN33]RXFP3. The BRET data were expressed as mean ± SE ($n = 3$) and fitted to $Y = B_{max}\ X/(X + K_d)$ for the data without competition or to a linear curve for the data with competition using the software SigmaPlot10.0. **b** Association and dissociation of R3/I5-S-CyOFP with living HEK293T cells overexpressing Luc-L8-[ΔN33]RXFP3. The data were fitted to $Y = B_{max}(1 - e^{-kX})$ for association or $Y = B_{max}e^{-kX}$ for dissociation using the software SigmaPlot10.0. **c** Competition binding of R3/I5 and INSL5 with Luc-L8-[ΔN33]RXFP3 using R3/I5-S-CyOFP as a tracer. The nonspecific binding was obtained by competition with 1.0 μM of R3/I5. The data were expressed as mean ± SE ($n = 3$) and fitted with sigmoidal curves using the software SigmaPlot10.0

had no detectable effects on the emission spectrum, suggesting that CyOFP did not bind to RXFP3.

Establishment of BRET-based ligand-binding assays for RXFP3

The results above suggested that R3/I5-S-CyOFP and Luc-L8-RXFP3 formed an efficient BRET pair. Next, we quantitatively measured their binding affinity through a saturation binding assay. As shown in Fig. 3a, the measured BRET data increased in a typical hyperbolic manner with increasing R3/I5-S-CyOFP concentration, suggesting saturation binding of the fluorescent tracer with the NanoLuc-fused receptor. Competition with 1.0 μM R3/I5 peptide almost completely abolished the BRET effect, confirming the measured BRET was derived from specific binding of R3/I5-S-CyOFP with Luc-L8-[ΔN33]RXFP3. The calculated dissociation constant (K_d) for the fluorescent tracer with the NanoLuc-fused shortened receptor was 2.60 ± 0.17 nM ($n = 3$), a value similar to those measured for intact human RXFP3 with ^{125}I-labeled, europium-labeled, or NanoLuc-conjugated R3/I5 tracers (in the range 1–5 nM). Thus, conjugation of CyOFP with R3/I5, fusion of NanoLuc with RXFP3, and removal of 33 N-terminal receptor residues had no detrimental effects on the binding of RXFP3 with R3/I5.

Contrast to conventional ligand–receptor binding assays, the BRET-based binding assay can conveniently monitor the ligand–receptor binding process in a real-time manner, because the unbound tracer does not interfere with the BRET measurement. As shown in Fig. 3b, after addition of NanoLuc substrate and R3/I5-S-CyOFP (final concentration 10 nM) to living HEK293T cells overexpressing Luc-L8-[ΔN33]RXFP3, the measured BRET data exponentially increased with a half-life of ~60 s, suggesting quick binding of the fluorescent tracer with the NanoLuc-fused receptor. After addition of R3/I5 peptide as a competitor (final concentration 1.0 μM), the measured BRET data exponentially decreased with a half-life of ~80 s, suggesting quick dissociation of the fluorescent tracer from the NanoLuc-fused receptor. Thus, the ligand-binding process of RXFP3 could be conveniently monitored in a real-time manner through the BRET-based binding assay.

Using the BRET pair of R3/I5-S-CyOFP and Luc-L8-[ΔN33]RXFP3, we established competition binding assays to quantitatively measure binding potencies of

various ligands with RXFP3. As shown in Fig. 3c, typical sigmoidal curves were obtained for both R3/I5 and INSL5, with calculated pIC_{50} values of 8.40 ± 0.04 for R3/I5 and 6.96 ± 0.03 for INSL5. Thus, R3/I5 displayed ~30-fold higher binding potency than INSL5 towards RXFP3 measured by the BRET-based binding assay. This binding potency difference was highly consistent with the value measured using the conventional binding assay on intact human RXFP3 (Hu et al. 2016a). Thus, binding potencies of various ligands with RXFP3 could be conveniently measured by the novel BRET-based binding assay.

The BRET-based ligand-binding assay for RXFP3 is convenient for use because it has just two simple steps. First, cells overexpressing the NanoLuc-fused receptor were mixed with the CyOFP-conjugated tracer (with or without competitor) and then incubated for ~10 min. Second, NanoLuc substrate was added and BRET data were measured on a plate reader. Owing to its simplicity, this binding assay can be easily adapted to automated high throughput screening using 96-well or 384-well plates. Thus, the BRET-based binding assay would facilitate interaction studies of RXFP3 with various ligands, such as characterization of designed agonists/antagonists or screening of novel ligands.

Application of the engineered CyOFP to other BRET-based binding assays

In the present study, we established a novel BRET-based ligand-binding assay for RXFP3 using the newly developed CyOFP as an efficient energy acceptor. The wild-type CyOFP has two intrinsic free Cys residues that can cause disulfide-linked aggregation and interfere with chemical conjugations based on thiol-disulfide exchange methodology. Thus, we generated an engineered CyOFP without the intrinsic Cys residues. The engineered CyOFP retained similar fluorescence properties to the wild-type protein, and thus it is a better version for BRET-based binding assays in future studies. To apply the engineered Cys-free CyOFP as an energy acceptor for the NanoLuc reporter, two approaches can be used to attach it to target molecules, such as proteins, peptides, carbohydrates or nucleic acids. One approach is chemical conjugation, that is, covalent crosslinking of the engineered CyOFP with purified target molecules through appropriate chemical reactions. The other approach is genetic fusion, that is, fusion of the engineered CyOFP gene with the gene of the target protein/peptide and overexpression of the fusion protein in suitable host cells. In future, the engineered Cys-free CyOFP will be widely used as an efficient energy acceptor for the NanoLuc reporter in various BRET-based interaction studies.

Acknowledgements This work was supported by grants from the National Natural Science Foundation of China (31470767, 31670773).

Compliance with ethical standards

Conflict of interest The authors declare that they have no conflict of interest.

Research involving human participants and/or animals This article does not contain any studies with human participants or animals performed by any of the authors.

References

Bathgate RA, Halls ML, van der Westhuizen ET, Callander GE, Kocan M, Summers RJ (2013a) Relaxin family peptides and their receptors. Physiol Rev 93:405–480

Bathgate RA, Oh MH, Ling WJ, Kaas Q, Hossain MA, Gooley PR, Rosengren KJ (2013b) Elucidation of relaxin-3 binding interactions in the extracellular loops of RXFP3. Front Endocrinol (Lausanne) 4:13

Bylund DB, Toews ML (2011) Radioligand binding methods for membrane preparations and intact cells. Methods Mol Biol 746:135–164

Callander GE, Bathgate RA (2010) Relaxin family peptide systems and the central nervous system. Cell Mol Life Sci 67:2327–2341

Calvez J, de Ávila C, Matte LO, Guèvremont G, Gundlach AL, Timofeeva E (2016) Role of relaxin-3/RXFP3 system in stress-induced binge-like eating in female rats. Neuropharmacology 102:207–215

Chu J, Oh Y, Sens A, Ataie N, Dana H, Macklin JJ, Laviv T, Welf ES, Dean KM, Zhang F, Kim BB, Tang CT, Hu M, Baird MA, Davidson MW, Kay MA, Fiolka R, Yasuda R, Kim DS, Ng HL, Lin MZ (2016) A bright cyan-excitable orange fluorescent protein facilitates dual-emission microscopy and enhances bioluminescence imaging in vivo. Nat Biotechnol 34:760–767

Gross LA, Baird GS, Hoffman RC, Baldridge KK, Tsien RY (2000) The structure of the chromophore within DsRed, a red fluorescent protein from coral. Proc Natl Acad Sci USA 97:11990–11995

Hall MP, Unch J, Binkowski BF, Valley MP, Butler BL, Wood MG, Otto P, Zimmerman K, Vidugiris G, Machleidt T, Robers MB, Benink HA, Eggers CT, Slater MR, Meisenheimer PL, Klaubert DH, Fan F, Encell LP, Wood KV (2012) Engineered luciferase reporter from a deep sea shrimp utilizing a novel imidazopyrazinone substrate. ACS Chem Biol 7:1848–1857

Halls ML, Bathgate RA, Sutton SW, Dschietzig TB, Summers RJ (2015) International Union of Basic and Clinical Pharmacology. XCV. Recent advances in the understanding of the pharmacology and biological roles of relaxin family peptide receptors 1–4, the receptors for relaxin family peptides. Pharmacol Rev 67:389–440

Haugaard-Kedström LM, Shabanpoor F, Hossain MA, Clark RJ, Ryan PJ, Craik DJ, Gundlach AL, Wade JD, Bathgate RA, Rosengren KJ (2011) Design, synthesis, and characterization of a single-chain peptide antagonist for the relaxin-3 receptor RXFP3. J Am Chem Soc 133:4965–4974

Hojo K, Hossain MA, Tailhades J, Shabanpoor F, Wong LL, Ong-Pålsson EE, Kastman HE, Ma S, Gundlach AL, Rosengren KJ, Wade JD, Bathgate RA (2016) Development of a single-chain peptide agonist of the relaxin-3 receptor using hydrocarbon stapling. J Med Chem 59:7445–7456

Hsu SY, Nakabayashi K, Nishi S, Kumagai J, Kudo M, Sherwood OD, Hsueh AJ (2002) Activation of orphan receptors by the hormone relaxin. Science 295:671–674

Hu MJ, Shao XX, Wang JH, Wei D, Guo YQ, Liu YL, Xu ZG, Guo ZY (2016a) Mechanism for insulin-like peptide 5 distinguishing the homologous relaxin family peptide receptor 3 and 4. Sci Rep 6:29648

Hu MJ, Shao XX, Wang JH, Wei D, Liu YL, Xu ZG, Guo ZY (2016b) Identification of hydrophobic interactions between relaxin-3 and its receptor RXFP3: implication for a conformational change in the B-chain C-terminus during receptor binding. Amino Acids 48:2227–2236

Hulme EC, Trevethick MA (2010) Ligand binding assays at equilibrium: validation and interpretation. Br J Pharmacol 161:1219–1237

Jayakody T, Marwari S, Lakshminarayanan R, Tan FC, Johannes CW, Dymock BW, Poulsen A, Herr DR, Dawe GS (2016) Hydrocarbon stapled B chain analogues of relaxin-3 retain biological activity. Peptides 84:44–57

Kuei C, Sutton S, Bonaventure P, Pudiak C, Shelton J, Zhu J, Nepomuceno D, Wu J, Chen J, Kamme F, Seierstad M, Hack MD, Bathgate RA, Hossain MA, Wade JD, Atack J, Lovenberg TW, Liu C (2007) R3(BDelta23-27)R/I5 chimeric peptide, a selective antagonist for GPCR135 and GPCR142 over relaxin receptor LGR7: in vitro and in vivo characterization. J Biol Chem 282:25425–25435

Kumagai J, Hsu SY, Matsumi H, Roh JS, Fu P, Wade JD, Bathgate RA, Hsueh AJ (2002) INSL3/Leydig insulin-like peptide activates the LGR8 receptor important in testis descent. J Biol Chem 277:31283–31286

Kumar JR, Rajkumar R, Jayakody T, Marwari S, Hong JM, Ma S, Gundlach AL, Lai MK, Dawe GS (2016) Relaxin' the brain: a case for targeting the nucleus incertus network and relaxin-3/RXFP3 system in neuropsychiatric disorders. Br J Pharmacol. doi:10.1111/bph.13564

Liu YL, Guo ZY (2016) Novel bioluminescent binding assays for interaction studies of protein/peptide hormones with their receptors. Amino Acids 48:1151–1160

Liu C, Chen J, Sutton S, Roland B, Kuei C, Farmer N, Sillard R, Lovenberg TW (2003a) Identification of relaxin-3/INSL7 as a ligand for GPCR142. J Biol Chem 278:50765–50770

Liu C, Eriste E, Sutton S, Chen J, Roland B, Kuei C, Farmer N, Jörnvall H, Sillard R, Lovenberg TW (2003b) Identification of relaxin-3/INSL7 as an endogenous ligand for the orphan G-protein-coupled receptor GPCR135. J Biol Chem 278:50754–50764

Liu C, Chen J, Kuei C, Sutton S, Nepomuceno D, Bonaventure P, Lovenberg TW (2005a) Relaxin-3/insulin-like peptide 5 chimeric peptide, a selective ligand for G protein-coupled receptor (GPCR)135 and GPCR142 over leucine-rich repeat-containing G protein-coupled receptor 7. Mol Pharmacol 67:231–240

Liu C, Kuei C, Sutton S, Chen J, Bonaventure P, Wu J, Nepomuceno D, Kamme F, Tran DT, Zhu J, Wilkinson T, Bathgate R, Eriste E, Sillard R, Lovenberg TW (2005b) INSL5 is a high affinity specific agonist for GPCR142 (GPR100). J Biol Chem 280:292–300

Luo X, Bathgate RA, Zhang WJ, Liu YL, Shao XX, Wade JD, Guo ZY (2010) Design and recombinant expression of insulin-like peptide 5 precursors and the preparation of mature human INSL5. Amino Acids 39:1343–1352

Ma S, Smith CM, Blasiak A, Gundlach AL (2016) Distribution, physiology and pharmacology of relaxin-3/RXFP3 systems in brain. Br J Pharmacol. doi:10.1111/bph.13659

Machleidt T, Woodroofe CC, Schwinn MK, Méndez J, Robers MB, Zimmerman K, Otto P, Daniels DL, Kirkland TA, Wood KV (2015) NanoBRET—a novel BRET platform for the analysis of protein–protein interactions. ACS Chem Biol 10:1797–1804

Maguire JJ, Kuc RE, Davenport AP (2012) Radioligand binding assays and their analysis. Methods Mol Biol 897:31–77

Shabanpoor F, Separovic F, Wade JD (2011) General method for selective labelling of double-chain cysteine-rich peptides with a lanthanide chelate via solid-phase synthesis. J Pept Sci 17:169–173

Shabanpoor F, Akhter Hossain M, Ryan PJ, Belgi A, Layfield S, Kocan M, Zhang S, Samuel CS, Gundlach AL, Bathgate RA, Separovic F, Wade JD (2012) Minimization of human relaxin-3 leading to high-affinity analogues with increased selectivity for relaxin-family peptide 3 receptor (RXFP3) over RXFP1. J Med Chem 55:1671–1681

Smith CM, Walker LL, Chua BE, McKinley MJ, Gundlach AL, Denton DA, Lawrence AJ (2015) Involvement of central relaxin-3 signalling in sodium (salt) appetite. Exp Physiol 100:1064–1072

Soave M, Stoddart LA, Brown A, Woolard J, Hill SJ (2016) Use of a new proximity assay (NanoBRET) to investigate the ligand-binding characteristics of three fluorescent ligands to the human β_1-adrenoceptor expressed in HEK-293 cells. Pharmacol Res Perspect 4:e00250

Stoddart LA, Johnstone EK, Wheal AJ, Goulding J, Robers MB, Machleidt T, Wood KV, Hill SJ, Pfleger KD (2015) Application of BRET to monitor ligand binding to GPCRs. Nat Methods 12:661–663

Subach OM, Malashkevich VN, Zencheck WD, Morozova KS, Piatkevich KD, Almo SC, Verkhusha VV (2010) Structural characterization of acylimine-containing blue and red chromophores in mTagBFP and TagRFP fluorescent proteins. Chem Biol 17:333–341

Sudo S, Kumagai J, Nishi S, Layfield S, Ferraro T, Bathgate RA, Hsueh AJ (2003) H3 relaxin is a specific ligand for LGR7 and activates the receptor by interacting with both the ectodomain and the exoloop 2. J Biol Chem 278:7855–7862

Yarbrough D, Wachter RM, Kallio K, Matz MV, Remington SJ (2001) Refined crystal structure of DsRed, a red fluorescent protein from coral, at 2.0-A resolution. Proc Natl Acad Sci USA 98:462–467

Zhang WJ, Luo X, Liu YL, Shao XX, Wade JD, Bathgate RA, Guo ZY (2012a) Site-specific DOTA/europium-labeling of recombinant human relaxin-3 for receptor-ligand interaction studies. Amino Acids 43:983–992

Zhang WJ, Luo X, Song G, Wang XY, Shao XX, Guo ZY (2012b) Design, recombinant expression and convenient A-chain N-terminal europium-labelling of a fully active human relaxin-3 analogue. FEBS J 279:1505–1512

Zhang L, Song G, Xu T, Wu QP, Shao XX, Liu YL, Xu ZG, Guo ZY (2013a) A novel ultrasensitive bioluminescent receptor-binding assay of INSL3 through chemical conjugation with nanoluciferase. Biochimie 95:2454–2459

Zhang WJ, Jiang Q, Wang XY, Song G, Shao XX, Guo ZY (2013b) A convenient method for europium-labeling of a recombinant chimeric relaxin family peptide R3/I5 for receptor-binding assays. J Pept Sci 19:350–354

Zhang C, Chua BE, Yang A, Shabanpoor F, Hossain MA, Wade JD, Rosengren KJ, Smith CM, Gundlach AL (2015) Central relaxin-3 receptor (RXFP3) activation reduces elevated, but not basal, anxiety-like behaviour in C57BL/6J mice. Behav Brain Res 292:125–132